Robust Design of a Novel Solar based Plug-in Electric Vehicle Scheme

Rao Muhammad Asif *, Ateeq Ur Rehman **, Subhashree Choudhury ***‡, Ismail Hossain ****, Muhammad Abu Bakar Siddiqui *, Taraprasanna Dash *****

* Department of Electrical Engineering, Superior University, Lahore 54000, Pakistan

** Department of Electrical Engineering, Government College University, Lahore 54000, Pakistan

*** Department of Electrical and Electronics Engineering, Siksha 'O' Anusandhan (Deemed to be University), Bhubaneswar, 751030, India

**** Ural Federal University, Department of Nuclear Power Plants & Renewable Energy, Yekaterinburg, Russia

***** Department of Electronics and Communication Engineering, Siksha 'O' Anusandhan (Deemed to be University), Bhubaneswar, 751030, India

(rao.m.asif@superior.edu.pk, ateqrehman@gmail.com, subhashreechoudhury@soa.ac.in, hossain.ismail44@yahoo.com, abu.bkr0110@gmail.com, taradash@soa.ac.in)

‡ Subhashree Choudhury, Bhubaneswar, 751030, India, Tel: +91-7008224930, subhashreechoudhury@soa.ac.in

Received: 13.06.2022 Accepted:29.07.2022

Abstract- Photovoltaic (PV) energy is the most desirable source because of its renewable and environment-friendly nature. This article presents a low-cost model of a solar-powered vehicle based on a Charging Management Controller (CMC). Fuzzy Logic Control (FLC) based Maximum Power Point Tracking (MPPT) technique is used for energy optimization and extraction of maximum power through the PV system. Furthermore, a DC series motor drive was used due to higher torque-speed characteristics with rheostat as a braking component for controlling the vehicle's speed. Even the AC plug-in socket is mounted to charge the batteries when the sunlight is unavailable. CMC is integrated with PV and AC plug-in to charge the battery bank and control the power transfer maintenance according to load side demand. It also prevents overcharging of batteries to increase their lifespan. The proposed model can satisfy the demand-supply ratio of EV by optimizing PV energy. It provides an economical and viable approach for designing hybrid, plug-in solar-powered electric vehicles.

Keywords Photovoltaic System; Maximum Power Point Tracking; Fuzzy Logic Control; Energy Storage; Renewable Energy Sources; Solar-powered Electric Vehicle.

1. Introduction

Solar Energy is the most desirable and viable renewable energy source (RES) to economically fulfil the increasing energy demand [1, 2]. Additionally, the PV system is maintenance-free in almost all aspects [3]. Furthermore, it has straightforward integration with Electric Vehicles (EVs) due to minimum energy conversion stages, and it has a noiseless, vibration-less, and smell-free mechanism. On the other hand, almost all internal combustion engine (ICE)-based vehicles use petrol, compressed natural gas, and crude oil worldwide as a source of energy [4]. Due to environmental risks, the engine technology should be replaced with alternate power sources that are more economical, highly efficient, and cause low emissions. Therefore, EVs and Hybrid Electric Vehicles (HEVs) alternate [5]. The PV system can be implemented by employing two approaches: PV-station type, i.e., installing the PV system on a power station for charging the vehicles; second is PV-standalone type, i.e., integrating PV module directly on the vehicles. Although hybrid EVs are accepted due to environment-friendly behaviour, these have not yet gained consumer's confidence due to certain technological shortcomings [6]. Therefore, in this paper, PV standalone

type is implemented on an EV in conjunction with plug-in modules for charging the battery bank.

Already, EV-related research exists in the literature, but no one has integrated a real-time prototype with the PV module [7]. Additionally, a control scheme related to solar-powered vehicles is reported [8] but not testified and updated. Furthermore, the limited surface area for integrating PV modules on EV is not applicable for auxiliary components. These issues motivated the authors to design and implement a PV system on EV for small applications, as illustrated in Figure 1 [9]. DC batteries are also employed for energy storage in abnormal weather profiles [10, 11]. The batteries used in this scheme have a high energy density, more reliable, and significant service life [8, 12]. A simulation model of the maximum power point tracking (MPPT) algorithm was introduced [13] and thus the engine's speed is maintained appropriately [14]. The DC series motor is used to control the vehicle's direction, i.e., forward or reverse, because of its better torque-speed characteristics. Rheostat speed control with the resistance control method is provided to control the motor speed. This also avoids the flow of excess current when the vehicle is supposed to stop or slow down, which is similar to conventional cars on fuel. In addition to this, it also deploys a small DC generator using a car radiator fan on the front side of the vehicle to generate power for lights, wipers, horns, and charging 50A battery.

Fig. 1. Basic schematic configuration of solar EVs

This article summarizes the design scheme of PV-EV and highlights further research potentials in the field of the PV system. After analysing the background history of different solar EVs, the results of this research agree well with the designed parameters, and the solar vehicle model is more capable than previous versions. Additionally, power quality monitoring techniques are reviewed to advance power management systems and the power industry.

2. Literature Review

EVs powered by PV systems, HEVs, and Plug-in Hybrid Electric Vehicles (PHEVs) are considered the most economically viable solutions. A remarkable fact is that EV was introduced in 1828, much earlier than the ICE vehicles. However, the ease in usage of ICE vehicles with higher driving capability, short time, and vast infrastructure of fuel refilling compared with the EV distracted users. Despite these advantages, ICE vehicles cannot be promoted due to severe environmental impacts and human health. Besides EV, a Global System for Mobile (GSM)-based realistic approach for remotely-controlled irrigation robots using PV energy is also proposed in [15, 16] instead of fossil fuels.

Many researchers have designed the charging unit for EVs. In this regard, a simulation-based mathematical model of improved MPPT with an interleaved boost converter is proposed for EVs charging [17]. In this system, a DC link is directly supplied from PV cells and DC batteries, and the interleaved DC/DC boost converter is placed between the supply of DC power and the DC link. This converter is placed for faster dynamic response and less stress on batteries. Furthermore, a passive element is placed to remove ripples from input current and output voltages, which is more efficient. However, this study has two limitations: power loss and harmonics due to switching noise during the power conversion process. The second one is that the induction motor's speed control is challenging [18].

An energy storage system is presented in [19] to optimize the PV energy of autonomous sail drones to enhance the efficiency and energy management of non-grid-connected applications, which is a very tough task. However, it significantly optimizes the storage energy by using a high-efficiency MPPT charger on each solar panel. Hydrogen assisted combustion engine powered by the solar system is proposed in [20]. Due to the severe dependency of the MPPT controller on weather conditions, it was considered a good initiative as the solar panel is used to produce Oxy-hydrogen (HHO) gas. Further, this gas was supplied to the combustion chamber of a well-efficient four-stroke diesel engine. This process also boosted the mixture process into the burning, which produces clean emissions. However, although it was a straightforward process where the 12V-50W solar panel is used, it also has some drawbacks, such as the flammability range and very high flame speed. Similarly, the partial usage of solar panels was a minor step and was not a permanent solution. So, researchers moved toward an efficient charging system by exploiting solar panels.

Another scheme was presented to improve the charging systems that describe EV charging functionality [21]. While the charging system for EVs was integrated with a grid station, it penetrated the grid. Therefore, this scheme needs bidirectional DC/DC converters and an MPPT panel for each PV string. Furthermore, a 10KW DC-DC charger was made for power generation from these PV strings. The charger was connected between a DC bus of the PV system and EV batteries coupled with a high pass filter to stop high transient from the inverter produced by the dynamic climatic profiles. Although simulation results expressed the capability to fast charge batteries using a PV system during conversion via bidirectional DC/DC converter. The output voltage has a minimal fluctuation called output noise, and this switching noise of converters causes harmonics. Similarly, small oscillation can also be observed in the transient response of the prescribed model with a DC/DC charger.

Still, there was a need for an efficient charging unit for the solar-powered electric vehicle (SEV) to charge the batteries efficiently and save battery life [22]. Therefore, studies proposed in [23] gave a solution of charging batteries for conventional vehicles. However, in this study, whenever the battery was going to be empty, these vehicles used another power source such as petrol, diesel, etc. So, it was more suitable for reducing fuels, but that was not a solar-based system and needed more improvement in the efficiency of the charging unit.

The proposed scheme in [21] was integrated with the PV grid, which caused the penetration of grids and the battery

bank. A charging unit model using the Arduino board was introduced for the parking zone to remove these penetrations, which enhanced the charging system for PHEVs and Photovoltaic Electric Vehicles (PEVs), as illustrated in Figure 2 [25]. It also modified the different communication technology for PHEVs and PEVs. This system also covered new and more flexible technologies like vehicle to grid, vehicle to the building, and smart charging. These technologies mentioned above paved the path for future researchers. This system removed the penetration on the grid, but the cost would increase when a separate solar system was placed for charging.

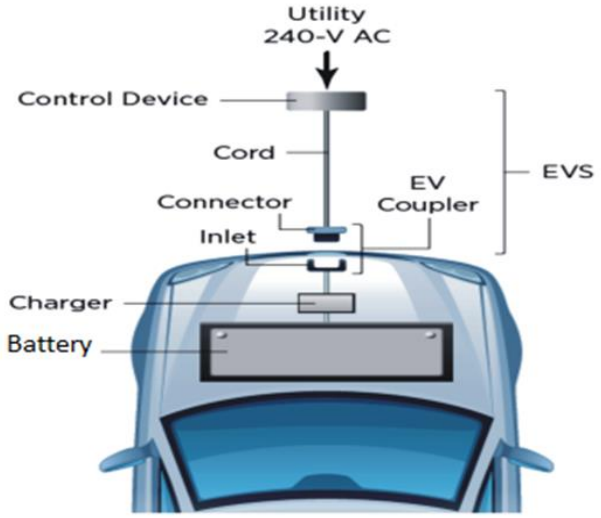

Fig. 2. Charging scheme for PHEVs [24]

In [23], the proposed design slightly affects the grid station and produces a harmonic that generates switching noise. Still, the model proposed in [24] removed this penetration effect but was costly. Therefore, a fuzzy logic power flow controller was introduced for the parking garage of PHEVs [26, 27]. That was based on five different charging priorities. The charging rates depend on the power of PV cells, the required power for PHEVs, and the cost of power. The controller was used to adjust the charging rate of PHEVs at different priorities levels, and it updates each PHEV with battery capacity and duration required for charging. It also predicted the upcoming power from PV cells and updated the charging/discharging of PHEVs [28]. Although this system removed all effects occurring in the on-grid station and compared PHEVs charging with and without a smart charging controller, the circuit was too complex, and the chance of failure increased due to complexity [29]. Furthermore, a robust Fuzzy Logic Controller (FLC) was reviewed to understand the MPPT technique better.

According to the previous study, a solar PV unit is proposed to charge the EVs in low voltage distribution grids [30]. This study shows that the loads unit becomes unpredictable due to high complexity and diverts the operating characteristics. The analysis of the combined effect of PV cells and EVs on residential grids resulted more intelligently if smart charges were used for low voltage grids. Therefore, a combined PV unit and EV integration model with two voltage residential grids, i.e., 630KVA and 400KVA are considered. Grid 1 consists of 166 householders and 6 feeders. Similarly, grid 2 consists of 75 householders and 5 feeders. This scheme was much feasible but lacked due to the often unavailability of the Sun. An effective plan for EV charging was modelled by introducing a smart controller to compensate for load during peak demands and bad weather conditions. However, there is a need to modify the transmission and distribution issues in this system.

PHEVs take charging decisions that depend on current rating, update energy prices after some time, and provide extra solar PV power to support any other grid [31]. Using the Electric Reliability Council of Texas (ERCOT) data, simulation results showed that the cost per day of energy PEV was $0.13, which was $50 per year. These sorts of PHEVs design were deployed on a large scale, and they made a substantial positive difference in the country's economy [32]. The merit of this design was that the PHEVs provided voltage support to distribution and updated the energy prices by managing electric power. However, there is a need to facilitate two systems in this design. The first one is the use of a universal communication model to update the voltage level of the system, and the second is the need for protection to increase battery life.

A scheduled system for charging the microgrids was introduced to avoid drawbacks experienced in [31]. The smart grid is integrated with solar panels, wind turbines, and the distribution grid. A controlling mechanism was also designed for the consumption by home appliances in which the remaining excess energy was utilized to charge the EV. Mix Integral Linear Programming (MILP) formulates the scheduled method, which enhances the reliability of power [33]. Charging the EVs with microgrids improves the efficiency and reliability of these systems. The performance increased with the scheduling scheme was almost 75% for 400 EVs and 85% for 590 EVs [34]. That was an efficient use of RES with a cost-effective energy generation. This design is mainly based on the charging of different vehicles. However, many vehicles are charged by the design mentioned above but have no particular scheme for charging flexibility. Besides, that model has errors in forecasting load consumption and power generation. The PHEV utilization model was proposed for researching flexibility for the charging scheme of EVs. In previous studies, EVs' variable load and RES generation fluctuations were significant concerns. Therefore, a power balancing between consumption and generation is the need for the current time. HEV is powered by an electric battery and a non-electrical source in this system. The model has provided information related to PHEV mobility, such as type of trip, change in duration, load charging, and use of only one fuel with the time function. Furthermore, a mathematical model is derived for EV utilization, electrical, fuel driving, flexible recharging, and price sensitivity. The results have expressed different charging units at parking sites resulting in a good impact on load profiles with the shifting of EV charging loads [35].

The proposed model is robust as it improves quality and reliability where the main contributions of this work are summarized as:

- A low-cost model of a solar-powered vehicle based on a Charging Management Controller (CMC) is taken into account.
- The proposed model efficiently optimized the Maximum Power Point Tracking (MPPT) technique for the PV panels used in the system.
- A DC series motor drive is deployed for higher torque-speed characteristics with rheostat as a braking component for controlling the vehicle's speed.
- CMC is integrated with PV and AC plug-in to charge the battery bank and control the power transfer maintenance according to load side demand, it increases the reliability
- The CMC is designed in such a way that it prevents overcharging of batteries to increase their lifespan.
- The proposed model can satisfy the demand-supply ratio of EV by optimizing PV energy. It provides an economical and viable approach for designing hybrid, plug-in solar-powered electric vehicles. The rest of the paper is organized as follows:

Section.2 summarizes the related work in electrical vehicles. Proposed Methodology is accomplished in section. 3. Section. 4 model and design where results and models design discussions are carried out. Section. The conclusion of the article is described in Section.5.

3. Proposed Methodology

In this paper, the PV module is configured to drive DC series motor using rheostat to control the proposed vehicle's speed. The FLC-based MPPT algorithm is used to track the maximum power of the PV module and reduce the fluctuations as well. Additionally, a 220V AC plug-in socket is also installed for charging the battery bank in case of weather concerns. The PV module and plug-in charging unit are coupled with a battery bank using a Charging Management Controller (CMC) to switch the power sources and maintain the state of charge (SOC) of batteries accordingly. During a bad climatic profile, the CMC will enable the plug-in charging mode. It also compares the available power and load demand for choosing the power source accordingly. Similarly, it maintains the 60% SOC and charging capacity of the battery. The controller also prevents the batteries from being overcharged. The DC series motor is employed on the tyres of the EV because of its higher torque-speed characteristics. To control the speed of the motor, the variable series resistance control method is proposed. The proposed design scheme of SEV is illustrated in Figure 3.

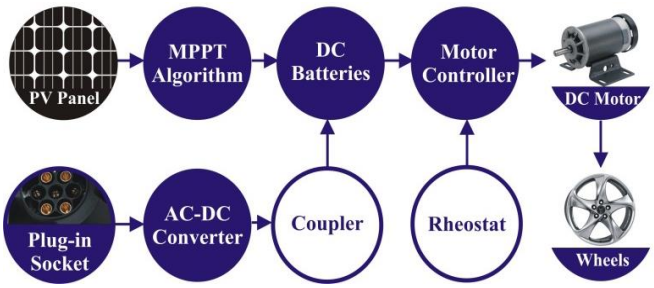

Fig. 3. The design scheme of the proposed vehicle

3.1. PV System

PV modules generate electricity by converting solar energy into electrical energy. Three types of PV modules are popular, i.e., polycrystalline, monocrystalline, and thin films, but monocrystalline is used to fulfil our energy needs in this work. A PV module has ratings of 250W with an open circuit DC voltage between 30-40V. The maximum efficiency is achieved by using blue antireflection silicon nitride where the solar cells are coated with it. The proposed methodology is given in Figure 4. Solar cell dimensions with electrical parameters are shown in Table 1.

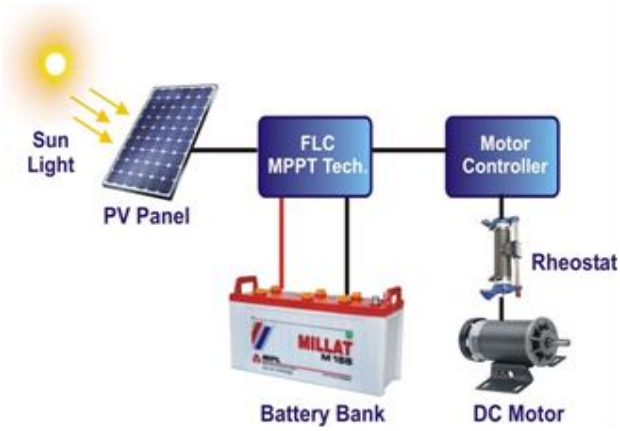

Fig. 4. Solar-powered DC motor control strategy

The PV current and voltage mainly rely on both irradiance and temperature. The mathematical model of the PV cell in terms of current and voltages is expressed by Equations (1) and (2) as

$$I = I_{ph} - I_o\left\{e^{\left[\frac{q_o}{nAKT}(V+nIR_s)\right]} - 1\right\} \quad (1)$$

$$V = \frac{nAKT}{q_o}\ln\left(\frac{I_{ph}+I_o-I}{I_o}\right) \quad (2)$$

The current and voltages are I, V, and K represents Boltzmann's constant. In addition, q_o and A are the electrical charge and ideality factor, respectively.

Voltage, current and power characteristics under different climate changes are observed in Figures 5(a) and 5(b), respectively. The PV module ratings are given in Table 1.

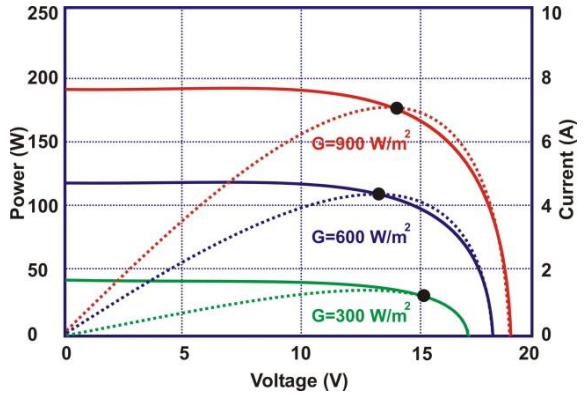

(A)

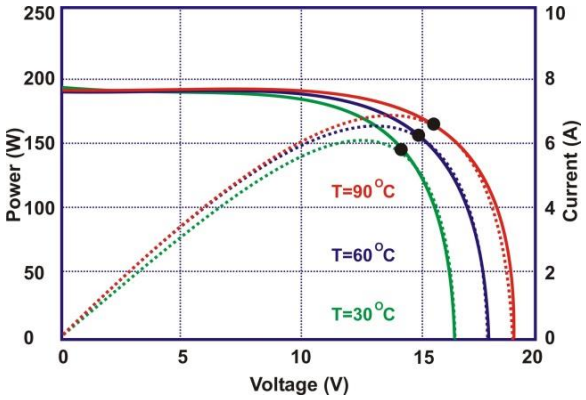

(B)

Fig. 5. The PV system's power-voltage and current characteristics: (A) at various irradiances; (B) at various temperatures

Table 1. Characteristics of the PV system

Characteristics	Ratings
PV cell size	156 × 156 mm
Number of cells in a module	60
Module weight	25 Kg
Power	250 W
Dimensions	1650 × 992 × 40 mm
Open circuit voltage	36 V
Maximum power voltage	33.3 V
Short circuit current	14.7 A
Maximum power current	13.67 A
Operating temperature	10 – 85 °C

3.2. FLC MPPT Algorithm

The FLC algorithm allocates parameter values to select appropriate fuzzy sets to optimize the output power of the PV system. First, it takes samples of V and I for optimal power calculation in each interval. The variation between the last instant and the current state is observed by considering the change of power and current rate. Similarly, a comparison was held between calculated and previous errors to get a change in error. Finally, both error and change in error are fed to the FLC as system inputs. FLC is used to drive the converter switches [13] as the switching through Pulse Width Modulation (PWM) controls the duty cycle. The observed power at an instant PE requires a large fuzzy step because the MPP is far from the optimal point. The modified algorithm for FLC is shown in Figure 6. The FLC algorithm optimizes the power by measuring the current output power level and comparing it with the previous fuzzy step, and then it declares the duty cycle accordingly.

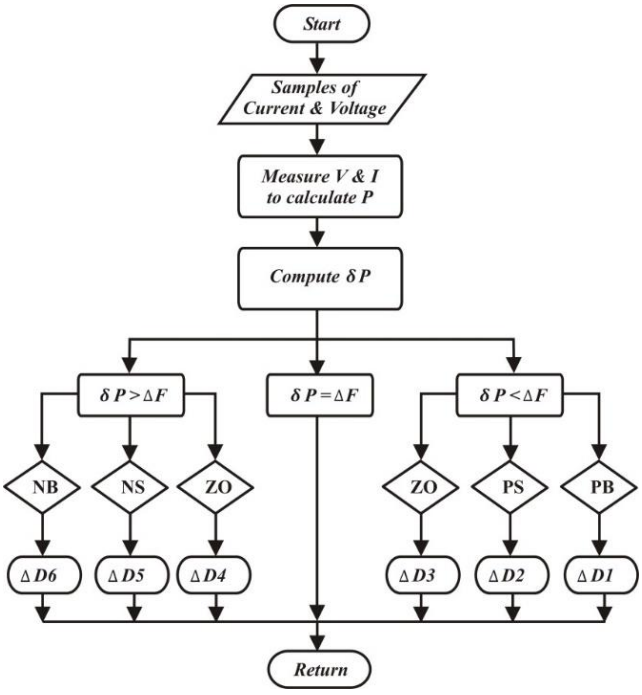

Fig. 6. Algorithm of modified FLC based MPPT

FLC algorithm follows the following rules for optimizing the power regarding Table 2 such as:

Rule 1: If $\delta P \gg \Delta F$, it means the current output power is far away from the old fuzzy step, therefore, negative big (NB) signal will be generated to process duty cycle ΔD6 as illustrated in Table 3.

Rule 2: If still $\delta P > \Delta F$ means the current value of output power has still not reached MPP, now it will process negative small (NS) signal for the generation of duty cycle ΔD5 as demonstrated in Table 3.

Rule 3: If $\delta P = \Delta F$ means current output power reached MPP, then it declares the same zero signal (ZO) to process the same duty cycle as the previous one.

Rule 4: If $\delta P \ll \Delta F$ means current output power is far away from the previous fuzzy step, therefore, positive big (PB) signal will be generated to process duty cycle ΔD1.

Rule 5: If still $\delta P < \Delta F$ means the current value of output

power is still away from MPP, now it will process a positive small (PS) signal for the generation of duty cycle ΔD2.

And so on. where δP is the instant power and ΔF is the fuzzy step.

Table 2. Fuzzy rules to optimize MPP

δP \ ΔF	Very Small	Small	Medium	Large	Very Large
Very Small	ZO	NS	NS	NB	NB
Small	PS	ZO	NS	NB	NB
Medium	PS	PS	ZO	NS	NB
Large	PB	PB	PS	ZO	NB
Very Large	PB	PB	PS	PS	ZO

Table 3. Duty cycle vs fuzzy rules

Duty Cycle	Value	Fuzzy Rule
ΔD1	D>0.5	PB
ΔD2	0.3<D<0.5	PS
ΔD3	0.1<D<0.3	ZO
ΔD4	-0.1<D<-0.3	ZO
ΔD5	-0.3<D<-0.5	NS
ΔD6	D>-0.5	NB

3.3. Battery Bank

This work uses lead-acid batteries because of cost-effectiveness, easy availability, and better capacity [36]. The PV system and plug-in charging are integrated with this battery bank. It is installed in the back trunk of a solar vehicle for better temperature and easy configuration to a plug-in socket. The battery has a 0.2Cn current for 5hr and 0.05Cn current for 20hr discharge, as presented in Figure 7. The battery's capacity depends on the discharge time, such as if the discharge time is longer, then the battery's capacity will be higher [37]. In our proposed model, a 100Ah battery is used with the applied current drawn from the panels being 14.7 amperes, as illustrated in Table 4. Equation (3) defines the charging time and the charging time for our battery bank is 6.80 hrs. as shown in Equation (4).

$$Charging\ T = \frac{Ah\ rating\ of\ the\ battery}{Applied\ Current} \quad (3)$$

$$Charging\ T = \frac{100Ah}{14.7A} = 6.80\ Hrs \quad (4)$$

Similarly, the motor used in this work is 1hp considering as the load consumes 746W. So, the discharging time of the battery bank can be obtained by using Equation (5) and the discharging time of our battery bank is 1.60 hrs. as presented in Equation (6).

$$Discharging\ T = \frac{Ah\ rating \times Voltage}{Applied\ Load} \quad (5)$$

$$Discharging\ T = \frac{100Ah \times 12V}{746W} = 1.60\ Hrs \quad (6)$$

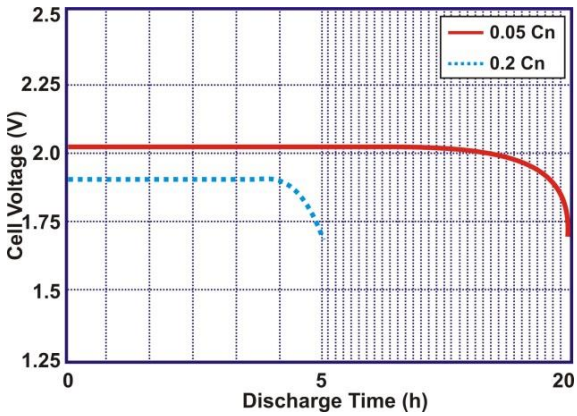

Fig. 7. Discharging behaviour of led acid battery for each cell

Table 4. Electrical Ratings for the battery bank

Characteristics	Ratings
Input Voltages	12 V
Input Current	14.7 A
Charging Ratting	100 Ampere hr
Time required for charging	6.8 hr
Electrical load	440 W
Time required for discharging	1.6 hr
Overall-Efficiency	≈82 %

3.4. Charging Management Controller

In this system, a 250W solar panel and plug-in charging socket are integrated with the battery bank on the input side for maintaining the SOC positive [38]. Similarly, a DC motor is configured on the load side that consumes electric power and discharges the battery bank. A CMC is proposed in this paper, which automatically disconnects the battery if it is going to be empty after getting the information about volts

and amperes of batteries, as illustrated in Figure 8. The followings are the steps of CMC.

- The active mode is ON when the power of the source is high as required, then the extra power is delivered to the battery bank to make the system reliable.
- On the other hand, if the power of the source is low as required, then then the extra power is supplied from the battery bank.

In addition, a threshold of 60% SOC is taken into account by CMC. It keeps the batteries in a healthy position. The lower level of SOC especially less than 10% reduces the battery life. The conditions which make the SOC within the limits are:

- The CMC will be considered in discharging state when SOC is lower than 60%. Meanwhile, it will be considered in the charging state when the SOC is greater than 60%.

E_c as charging energy based on SOC is defined in Equations (7) and (8).

$$E_c = \delta(SOC)_B \times C_B \tag{7}$$

$$SOC = SOC(t_o) - \frac{\int_{t_0}^{t} i_b(t)dt}{C_B \times 3600} \tag{8}$$

Where $\delta(SOC)_B$ is the change in SOC of the battery, C_B is the capacity of the battery, and i_b is the charging current of the battery.

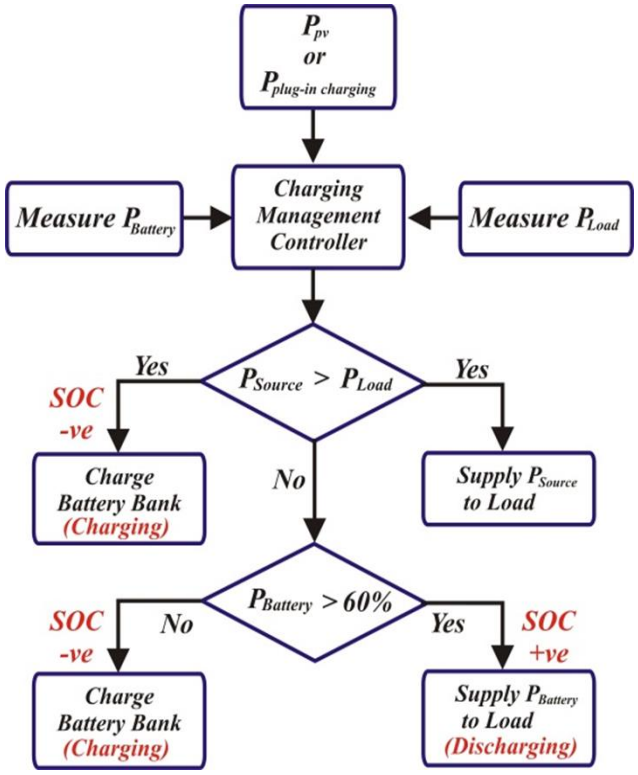

Fig. 8. Flow chart of the CMC

3.5. DC Series Motor

The DC series motor is coupled with the tyres of the electric vehicle to control the drive system efficiently. Moreover, it is integrated with the PV system as the primary source and battery bank as a backup in bad weather conditions. The main advantage of using a DC series motor is that it can securely handle the inrush currents since the motor does not function for an extended period. It also results in maximum active torque on the employment of different load torques [39]. Because of this, the DC series motor is preferred as it can drive the vehicle easily.

In the proposed scheme, the DC series motor is connected with a voltage source of CMC to operate on the main supply obtained from the PV system and a backup supply from the battery bank. The speed controller generates the duty cycle after comparing the reference speed and the motor's actual speed, then the boost converter applies a control signal to drive the motor. The speed and torque of the motor are controlled accordingly. The schematic block diagram of the integrated series motor is presented in Figure 9.

A DC motor of 2hp is used as a vehicle drive in this work. The output speed (rpm), output electrical power, and input electrical power of the DC series motor can be obtained by using Equations (9), (10), and (11), respectively.

$$P_{o\,(rpm)} = \frac{2\pi N T_{sh}}{60 \times 746} \tag{9}$$

$$P_{out} = HP \times 0.746\ KW \tag{10}$$

$$P_{in\,(E)} = \frac{P_{out}}{\eta} \tag{11}$$

According to Equation (15), the motor provides an output power of 1.5KW on full load. Taking η = 82% from the datasheet of the DC series motor, using Equation (16), we required 1.83KW power to drive the DC motor at the rated speed. Based on the electrical and mechanical subsystems of a series DC motor, mathematical modelling in terms of differential equations can be expressed as Equations (12) and (13) [9].

$$V(t) = Ri(t) + L\frac{di(t)}{dt} + k_o\omega(t)i(t) \tag{12}$$

$$T_e(t) = T_L(t) + b\omega(t) + J\frac{d\omega(t)}{dt} \tag{13}$$

where $\omega(t)$ = rotor speed, $T_L(t)$ = load torque, b = friction coefficient, J = rotor inertia, and $Te(t)$ = electromagnetic torque produced by the motor

In the following subsections, some characteristics are discussed to meet the solar vehicle requirements.

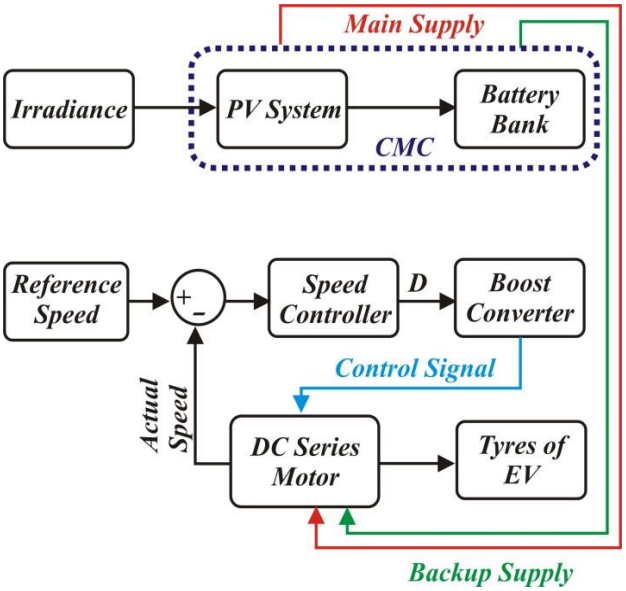

Fig. 9. Schematic flow chart of DC series motor

3.5.1. Torque Characteristics

As vehicle requires high torque in starting and a stabilized torque after some time when it moves smoothly. The studies on series motors comprise the same torque characteristics as presented in Figure 10 due to the direct relation of torque with both armature current and flux density as stated in Equation (14).

$$T \propto \varphi \propto I_A \tag{14}$$

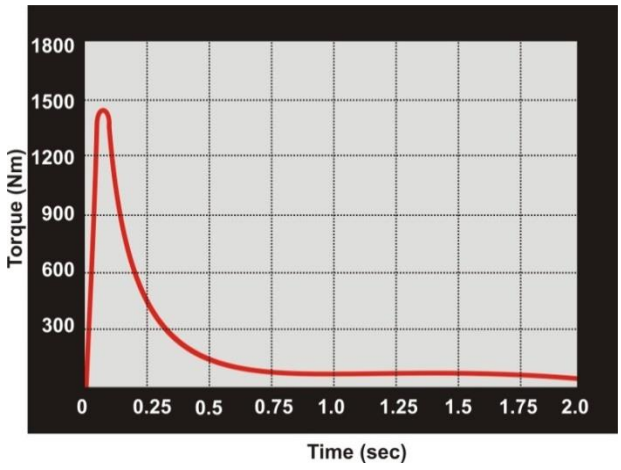

Fig. 10. Torque characteristics of series DC motor

3.5.2. Armature Current Characteristics

According to Equation (19), it is clear that the high starting torque causes a high armature current, so it meets our requirements very well. Moreover, in running conditions, it will be stable, as shown in the simulation result of Figure 11.

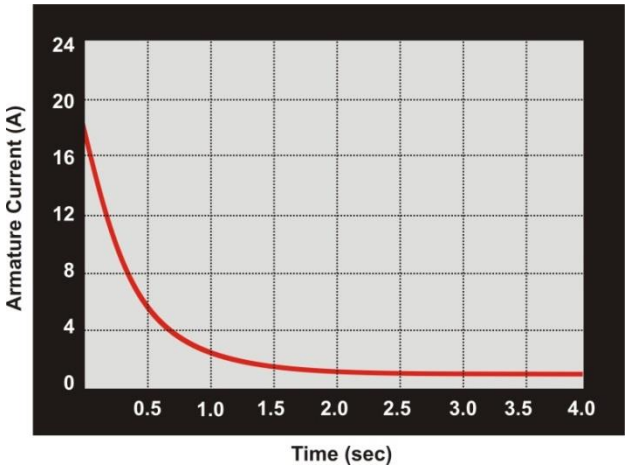

Fig. 11. Armature current characteristics

3.5.3. Speed Characteristics

The vehicle's speed will rise almost exponentially as speed and torque have an inverse relation. While starting, its speed slowly rises, and after the stability of torque, speed increases smoothly, as illustrated in Figure 12. It is also feasible for heavy load applications that need more torque and slow speed while starting.

If the flux decreases, the motor speed grows, but the motor torque decreases as stated in Equations (15) and (16). This is not probable because the increase in motor speed must result in better torque. Indeed, it is so in this circumstance. When the flux decreases, the armature current increases to a considerable value. As a result, despite the declining field, the torque is momentarily enlarged to a high-value end that will exceed the value matching considerably to the load. A lab experiment is also conducted to visualize the behaviour of the DC series motor, as illustrated in Figure 13.

$$N = \frac{K(V - I_A R_a)}{\phi} \tag{15}$$

$$N = \frac{K E_b}{\phi} \tag{16}$$

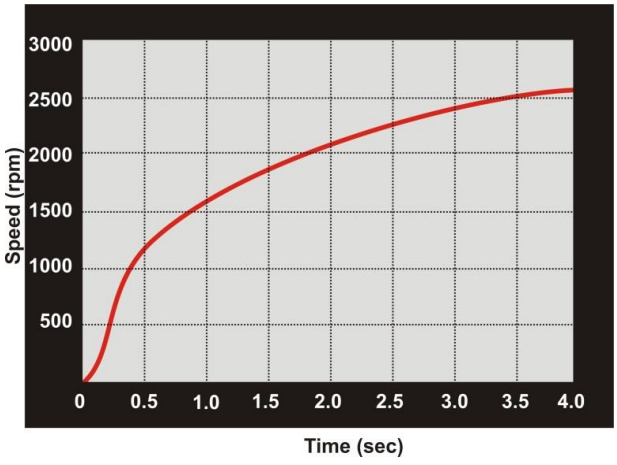

Fig. 12. Speed characteristics of series DC motor

(A)

(B)

(C)

(D)

Fig. 13. A lab experiment of the series DC motor: (A) operating voltage; (B) speed of the motor at 1.27 amperes; (C) speed of the motor at 6.41 amperes; (D) speed of the motor at 14.7 amperes

Table 5. Current-speed characteristics of DC series motor

Current	Speed
1.27 A	343 rpm
6.41 A	1332 rpm
14.7 A	2976 rpm

The results show that the selected motor has excellent performance at given requirements. For example, it has a shorter response time, very small overshoot, and no steady-state error. Table 6 illustrates the DC motor parameters used in this proposed model.

Table 6. Parameters of DC series motor

Characteristics	Ratings
Rated horsepower	2 hp
Rated current	130 A
Rated supply voltage	12 V
Rated speed	3000 rpm
Power at rated load	1.83 KW
Maximum torque	1480 Nm
Armature winding resistance	3.76 Ω
Armature winding inductance	0.06 H
Field winding resistance	250 Ω
Field winding inductance	110 H
Rotor inertia	0.035 kgm^2
Rotor damping ratio	0.2
Resistance temperature coefficient	0.0040 Ω/°C
Efficiency	82

3.6. Braking System

Sometimes abrupt braking may be applied to stop a DC motor very rapidly. There are two approaches, i.e., mechanical or electrical braking, to stop/slow down the speed of a running motor. In mechanical braking, a brake shoe applies friction on the moving tyres to halt or slow down the vehicle. In this method, the dissipation of the kinetic energy of the motor occurs in the form of heat. Similarly, in electrical braking, a rheostat is used to obstruct the flow of electric current, and the dissipation of kinetic energy occurs in resistance as heat [18]. The horsepower

established by the shaft torque is known as brake horsepower (BHP). If the motor is running and the shaft torque is T (Nm), then work done on each revolution and work done per minute of the DC motor can be calculated from Equations (17) and (18). Also, useful horsepower can be obtained using Equation (19).

$$\frac{W.D}{Revolution} = F \times 2 \times \pi \times r = 2 \times \pi \times T \quad (17)$$

$$\frac{W.D}{minute} = 2 \times N \times T \quad (18)$$

$$Useful\,P_{out} = 2 \times \pi \times N \times \frac{Tsh}{60 * 746}\,HP \quad (19)$$

Therefore, the rheostat controls the speed of the motor by using the resistance control method. It can overcome the excess flow of the current when the vehicle is supposed to stop or slow down [40], when the resistance increases in series with the motor, that decreases the applied voltage, which reduces the speed. In this way, a rheostat in series with the armature is deployed to vary the resistance to vary the speed ultimately.

3.7. Efficiency of the DC Motor

Like a DC generator, the efficiency of a DC motor is the relation of output power to the input power, i.e., Equation (20).

$$\eta = \left(\frac{Output}{Input} + Losses\right) * 100 \quad (20)$$

According to its datasheet, the motor used in this work has 82% overall efficiency. The power stages in a DC motor are characterized by copper losses between A-B and iron or friction losses between B-C, as expressed in Figure 14.

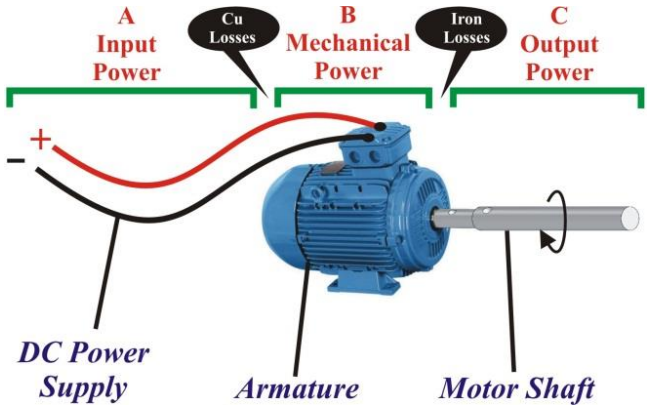

Fig. 14. Power stages of the DC motor

Therefore, the mechanical and overall efficiency of the DC motor can be evaluated by using Equations (21) and (22), respectively.

$$\eta_{mechanical} = \frac{B}{A} + Cu\,Losses * 100 \quad (21)$$

$$\eta_{overall} = \frac{C}{A} + Losses * 100 \quad (22)$$

4. Model and Design

Mechanical design plays a vital role in components adjustment fittings and customer's choice for an efficient vehicle. All electrical and mechanical components will only work if adjusted adequately against appropriate dimensions. A 250W monocrystalline PV panel can be installed on the car's roof using Very High Bond (VHB) double-sided instant bonding tape for a smooth and clean visual appearance. The back trunk of the car can be used as a battery bank in which a CMC and two parallel-connected 130A batteries are placed in a safe and secure position. A plug-in charging socket is installed in a fuel injecting place for easy connectivity with CMC to recharge the battery bank. The alternator's output power charges a 50A battery inside the car bonnet. This power is utilized for all auxiliary components of the vehicle. All the mechanical components, including ICE, radiator, air filter, etc., are extracted for the DC series motor placement with gear-box and wheels. The speed of the motor is controlled using rheostat by limiting the applied current of the DC motor, as stated in Figure 15.

DC motor in replacement of ICE engine coupled with an automatic transmission gear-box of the car for smooth and better torque-speed characteristics under load conditions. Similarly, this model can also utilize the extracted radiator fan and alternator for energy generation. This power is used to charge the 50A battery and is also utilized for small components such as headlights, indicators, horns, wipers, and car fans. The back trunk of the car is used as a secured place for the battery bank and other components. Both parallel-connected 130A batteries and CMC are configured in the vehicle's trunk to maintain operating temperature and the specification of the proposed model are presented in Table 7. Additionally, the fuel injecting portion of the car is used to charge externally using a plug-in charging socket, as shown in Figure 15. The proposed model of the novel RES-based plug-in EV's top view is shown in Figure 15. The model presented in [41] is deployed where the starting current is reduced while our models consist of CMC. It improved the charging infrastructure due to multi-sources such as PV and a plug-in charging scheme. The SOC of the battery is monitored, it declares some decisions to switch power sources according to the requirement of the system and considerations regarding battery lifetime. Although the hardware specifications presented in [41] have high capacity but our model is comparatively improved electrical parameters as shown in table.7.

The proposed robust design of a novel solar-based plug-in electric vehicle has efficiently improved the vehicle performance as compared to existing solar vehicles like [31,39,41] in terms of a better charge controller that increases the battery life and charging time, mileage is high if the model comparatively enhanced, supporting starting current characteristics, and an upgraded SOC system.

Table 7. Specifications and dimensions of the proposed model

Parameters	Ratings
Vehicle size	3800 x 1650 x 1240 mm
Wheel track	2 feet
Wheelbase	1 foot 7 inches
Tyre size	130/60-10
Load bearing capacity	~ 450 Kg
Seat capacity	4
Mileage	~ 55 Km
Vehicle maximum speed	60 Km/h
Brake type	Mechanical (Disc)
Brake system	Both foot and hand
Battery	12 V, 260 Ah
No. of batteries	2
Battery weight	~ 75 Kg
PV module weight	~ 20 Kg
Motor type	DC Brushless Series
DC motor weight	6 Kg
Motor horsepower	2 hp
Plug-in charger	220V AC
Charging time	~ 6-8 h
Vehicle weight	~1200 Kg

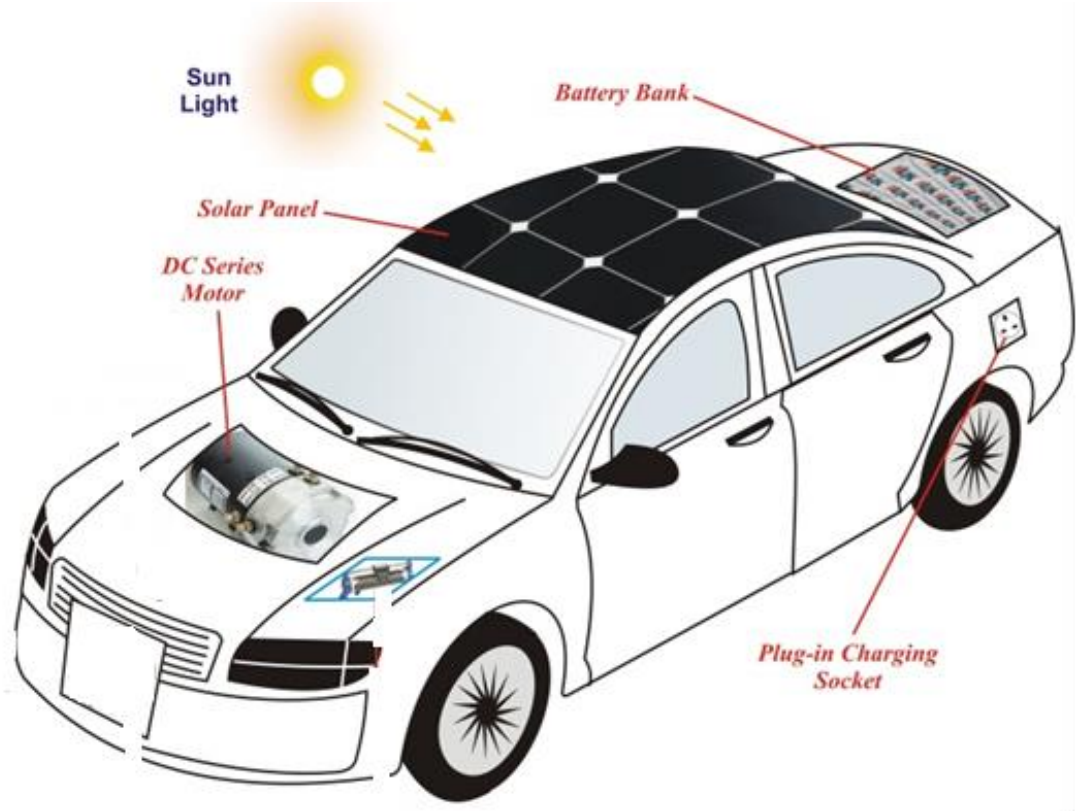

Fig. 15. Components assembling position in EV

5. Conclusion

Integrating PV systems in EVs remarkably reduces global warming, environmental impacts, and air pollution risks. Furthermore, using EVs instead of conventional vehicles provides more reliability and a much more inexpensive means of transportation. The proposed design presented in this article is mathematically modelled for simulations and hardware implementation. The FLC-based MPPT methodology expressed efficient behaviour for power extraction through the PV system. The configuration of the CMC improved the charging infrastructure due to multi-sources such as PV and a plug-in charging scheme. Based on the SOC of the battery, it declares some decisions to switch power sources according to the requirement of the system and considerations regarding battery lifetime. The feasibility and suitability of the DC series motor are also considered in the realistic model of the proposed vehicle. To employ an appropriate braking system, a rheostat is configured on the motor drive to stop or slow down the vehicle's speed.

References

[1] S. Choudhury and P. K. Rout. "Adaptive Fuzzy Logic Based MPPT Control for PV System under Partial Shading Condition." International Journal of Renewable Energy Research (IJRER) 5.4 (2015): 1252-1263., doi: 10.1109/TEC.2004.827719.

[2] A. R. Bhatti, Z. Salam, M. J. B. A. Aziz, and K. P. Yee, "A critical review of electric vehicle charging using solar photovoltaic," International Journal of Energy Research, vol. 40, no. 4, pp. 439–461, Mar. 2016, doi: 10.1002/er.3472.

[3] M. Akil, E. Dokur and R. Bayindir, "A Systematic Data-driven Analysis of Electric Vehicle Electricity Consumption with Wind Power Integration," 2021 10th International Conference on Renewable Energy Research and Application (ICRERA), 2021, pp. 397-401, doi: 10.1109/ICRERA52334.2021.9598483.

[4] Sahoo, Gagan Kumar, et al. "Recent Trends and Topology of Electric Vehicle Charging through DC Microgrid." 2022 IEEE Delhi Section Conference (DELCON). IEEE, 2022.

[5] M. Waseem, A. F. Sherwani, and M. Suhaib, "Integration of solar energy in electrical, hybrid, autonomous vehicles: a technological review," SN Applied Sciences, vol. 1, no. 11, 2019, doi: 10.1007/s42452-019-1458-4.

[6] I. Mohiuddin, A. Almogren, M. Al Qurishi, M. M. Hassan, I. Al Rassan, and G. Fortino, "Secure distributed adaptive bin packing algorithm for cloud storage," Future Generation Computer Systems, 2019, doi: 10.1016/j.future.2018.08.013.

[7] S. Choudhury. "Review of energy storage system technologies integration to microgrid: Types, control strategies, issues, and future prospects." Journal of Energy Storage 48 (2022): 103966.

[8] J. V. Vas, S. Venugopal, and V. G. Nair, "Control scheme for electrical drive of solar powered vehicles," Proceedings of the INDICON 2008 IEEE Conference and Exhibition on Control, Communications and Automation, vol. 1, pp. 75–80, 2008, doi: 10.1109/INDCON.2008.4768804.

[9] A. Hassan, A. U. Rehman, N. Shabbir, S. R. Hassan, M. T. Sadiq, and J. Arshad, "Impact of inertial response for the variable speed wind turbine," in 2019 International Conference on Engineering and Emerging Technologies, ICEET 2019, May 2019, doi: 10.1109/CEET1.2019.8711826.

[10] S. Choudhury, et al. "A supervisory state of charge and state of power management control strategy among hybrid energy storage systems through thermal exchange optimization technique." 2020 IEEE Calcutta Conference (CALCON). IEEE, 2020, doi: 10.1109/CALCON49167.2020.9106560.

[11] Cetinkaya, Umit, Ramazan Bayindir, and Samet Ayik. "Ancillary Services Using Battery Energy Systems and Demand Response." 2021 9th International Conference on Smart Grid (icSmartGrid). IEEE, 2021.

[12] S. Choudhury, N. Khandelwal, and A. Satpathy. "A Robust Competitive Optimization Algorithm Based Energy Management Control Strategy in a Battery and Ultracapacitor Based Hybrid Energy Storage System." Advances in Electrical Control and Signal Systems. Springer, Singapore, 2020. 1049-1066., doi: 10.1007/978-981-15-5262-5_81.

[13] R. M. Asif et al., "Design and analysis of robust fuzzy logic maximum power point tracking based isolated photovoltaic energy system," Engineering Reports, Jul. 2020, doi: 10.1002/eng2.12234.

[14] Y. Yuan, T. Q. Liu, Q. Li, and X. Y. Zhou, "A new maximum power point tracking algorithm for solar vehicle," in Asia-Pacific Power and Energy Engineering Conference, APPEEC, 2012, doi: 10.1109/APPEEC.2012.6307192.

[15] A. U. Rehman, R. M. Asif, R. Tariq, and A. Javed, "Gsm based solar automatic irrigation system using moisture, temperature and humidity sensors," in 2017 International Conference on Engineering Technology and Technopreneurship, ICE2T 2017, Dec. 2017, vol. 2017-Janua, pp. 1–4, doi: 10.1109/ICE2T.2017.8215945.

[16] R. A. Naqvi, M. Arsalan, A. Rehman, A. U. Rehman, W.-K. Loh, and A. Paul, "Deep Learning-Based Drivers Emotion Classification System in Time Series Data for Remote Applications," Remote Sensing, vol. 12, no. 3, p. 587, Feb. 2020, doi: 10.3390/rs12030587.

[17] F. Khoucha, A. Benrabah, O. Herizi, A. Kheloui, and M. E. H. Benbouzid, "An improved MPPT interleaved boost converter for solar electric vehicle application," in International Conference on Power Engineering, Energy and Electrical Drives, 2013, doi: 10.1109/PowerEng.2013.6635760.

[18] S. Sharma, S. S. Oberoi, and S. Nair, "Speed Control Method OF DC series motor," INTERNATONAL JOURNAL OF INNOVATIVE RESEARCH IN TECHNOLOGY, IJIRT, vol. vol1, no. issue:6, p. pp 1450-1453, 2014.

[19] E. Boni, M. Montagni, A. Moreschi, and L. Pugi, "Energy Storage System optimization for an Autonomous SailBoat," in 5th International Forum on Research and Technologies for Society and Industry: Innovation to Shape the Future, RTSI 2019 - Proceedings, Sep. 2019, pp. 231–235, doi: 10.1109/RTSI.2019.8895512.

[20] N. S. Jamoshid, N. H. Hashim, R. B. Ali, and N. S. Saudin, "Solar-operated hydrogen assisted combustion using solar PV panel to reduce vehicle's fuel consumption," in Proceedings of the 2013 IEEE 7th International Power Engineering and Optimization Conference, PEOCO 2013, 2013, doi: 10.1109/PEOCO.2013.6564531.

[21] Akil, Murat, Emrah Dokur, and Ramazan Bayindir. "Impact of electric vehicle charging profiles in data-driven framework on distribution network." 2021 9th International Conference on Smart Grid (ICSMARTGRID). IEEE, 2021.

[22] Asif, Rao Muhammad, et al. "Increase battery time by improvement in regenerative braking with storage system in hybrid vehicle." Journal of Applied and Emerging Sciences 9.1 (2019): pp-53.

[23] A. Brissette, A. Hoke, J. Traube, F. Lu, and D. Maksimovizc, "Study on the effect of solar irradiance intermittency mitigation on electric vehicle battery lifetime," in 2013 1st IEEE Conference on Technologies for Sustainability, SusTech 2013, 2013, doi: 10.1109/SusTech.2013.6617331.

[24] R. A. Benela and K. Jamuna, "Design of charging unit for electric vehicles using solar power," in International Conference on Information Communication and Embedded Systems, ICICES, 2013, doi: 10.1109/ICICES.2013.6508236.

[25] A. M. Furqan Durrani, A. U. Rehman, A. Farooq, J. A. Meo, and M. T. Sadiq, "An automated waste control management system (AWCMS) by using Arduino," in 2019 International Conference on Engineering and Emerging Technologies, ICEET 2019, 2019, doi: 10.1109/CEET1.2019.8711844.

[26] E. Radwan, M. Nour, E. Awada, and A. Baniyounes, "Fuzzy Logic Control for Low-Voltage Ride-Through Single-Phase Grid-Connected PV Inverter," Energies, vol. 12, no. 24, p. 4796, Dec. 2019, doi: 10.3390/en12244796.

[27] T. Ma and O. A. Mohammed, "Optimal charging of plug-in electric vehicles for a car-park infrastructure," in IEEE Transactions on Industry Applications, 2014, doi: 10.1109/TIA.2013.2296620.

[28] I. S. Alkhalifa and A. S. Almogren, "NSSC: Novel Segment Based Safety Message Broadcasting in Cluster-Based Vehicular Sensor Network," IEEE Access, 2020, doi: 10.1109/ACCESS.2020.2974157.

[29] A. S. Almogren, "Developing a Powerful and Resilient Smart Body Sensor Network through Hypercube Interconnection," International Journal of Distributed Sensor Networks, 2015, doi: 10.1155/2015/609715.

[30] J. R. Pillai, S. H. Huang, B. Bak-Jensen, P. Mahat, P. Thogersen, and J. Moller, "Integration of solar photovoltaics and electric vehicles in residential grids," in IEEE Power and Energy Society General Meeting, 2013, doi: 10.1109/PESMG.2013.6672215.

[31] J. M. Foster, G. Trevino, M. Kuss, and M. C. Caramanis, "Plug-in electric vehicle and voltage support for distributed solar: Theory and application," IEEE Systems Journal, 2013, doi: 10.1109/JSYST.2012.2223534.

[32] A. Almogren, "An automated and intelligent Parkinson disease monitoring system using wearable computing and cloud technology," Cluster Computing, 2019, doi: 10.1007/s10586-017-1591-z.

[33] F. Khan, M. A. B. Siddiqui, A. U. Rehman, J. Khan, M. T. S. A. Asad, and A. Asad, "IoT Based Power Monitoring System for Smart Grid Applications," in 2020 International Conference on Engineering and Emerging Technologies (ICEET), 2020, pp. 1–5, doi: 10.1109/ICEET48479.2020.9048229.

[34] H. Jin, S. H. Nengroo, S. Lee and D. Har, "Power Management of Microgrid Integrated with Electric Vehicles in Residential Parking Station," 2021 10th International Conference on Renewable Energy Research and Application (ICRERA), 2021, pp. 65-70, doi: 10.1109/ICRERA52334.2021.9598765.

[35] A. U. Rehman, R. A. Naqvi, A. Rehman, A. Paul, M. T. Sadiq, and D. Hussain, "A Trustworthy SIoT Aware Mechanism as an Enabler for Citizen Services in Smart Cities," Electronics, vol. 9, no. 6, 2020, doi: 10.3390/electronics9060918.

[36] S. Choudhury, and N. Khandelwal. "A Novel Weighted Superposition Attraction Algorithm-based Optimization Approach for State of Charge and Power Management of an Islanded System with Battery and SuperCapacitor-based Hybrid Energy Storage System." IETE Journal of Research (2020): 1-14., doi: 10.1080/03772063.2020.1839360.

[37] Jan, Khadim Ullah, et al. "Experimental Evaluation of the True Remaining Capacity of Legacy Lead-Acid Batteries." 2021 9th International Conference on Smart Grid (icSmartGrid). IEEE, 2021.

[38] F. L. Mapelli, D. Tarsitano, and M. Mauri, "Plug-in hybrid electric vehicle: Modeling, prototype realization, and inverter losses reduction analysis," IEEE Transactions on Industrial Electronics, 2010, doi: 10.1109/TIE.2009.2029520.

[39] Z. Bitar, A. Sandouk, and S. Al Jabi, "Testing the Performances of DC Series Motor Used in Electric Car," Journal of Energy Procedia, vol. vol 74, p. pp 148-159, 2015, doi: 10.1016/j.egypro.2015.07.536.

[40] M. Ernest, "Speed Control of DC Shunt Motor with Field and Armature Rheostat Control Simultaneously," Advance in Electronic and Electric Engineering, vol. vol 3, p. pp 77-80, 2013.

[41] Baghel, Rahul, Ghritlahre, Harish Kumar, Patel, Ram Narayan, Sahu, Ankit, Patel, Ashish and Verma, Mukesh Kumar. "Design and performance improvements of solar based efficient hybrid electric vehicle" International Journal of Emerging Electric Power Systems, vol. , no. , 2021, pp. 000010151520210247. https://doi.org/10.1515/ijeeps-2021-0247